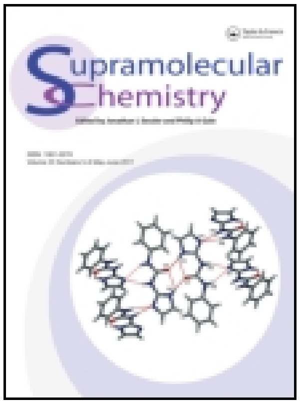

Supramolecular Chemistry
Publication details, including instructions for authors and subscription information:
http://www.tandfonline.com/loi/gsch20

Hydrogen-bonded chains formed by 5,5-diethylbarbituric acid and bipyridyl tectons

Emma Golden [a], Stephen P. Argent [a], Alexander J. Blake [a], Frédéric Thébault [a] & Neil R. Champness [a]

[a] School of Chemistry, University of Nottingham, University Park, Nottingham, NG7 2RD, UK

To cite this article: Emma Golden, Stephen P. Argent, Alexander J. Blake, Frédéric Thébault & Neil R. Champness (2012): Hydrogen-bonded chains formed by 5,5-diethylbarbituric acid and bipyridyl tectons, Supramolecular Chemistry, 24:1, 40-47

To link to this article: http://dx.doi.org/10.1080/10610278.2011.622383

Supramolecular Chemistry
Vol. 24, No. 1, January 2012, 40–47

Hydrogen-bonded chains formed by 5,5-diethylbarbituric acid and bipyridyl tectons

Emma Golden, Stephen P. Argent, Alexander J. Blake, Frédéric Thébault and Neil R. Champness*

School of Chemistry, University of Nottingham, University Park, Nottingham NG7 2RD, UK

(*Received 16 June 2011; final version received 7 September 2011*)

Supramolecular interactions play an important role in determining the solid-state structures of many molecular species. In this study, we describe the role of pyridyl-based molecules in forming hydrogen-bonded chains with 5,5-diethylbarbituric acid (DEB). The single crystal X-ray structures of three hydrogen-bonded co-crystals all exhibit one-dimensional chains formed *via* N—H···N interactions between pyridyl hydrogen bond acceptors and N—H hydrogen bond donors of DEB. Subtle differences are observed between the three related co-crystals. Although both DEB·4,4'-bipy, **1**, and DEB·diaz, **2**, (diaz = 2,7-diazapyrene) adopt similar one-dimensional chains with a 1:1 DEB:bipyridyl stoichiometry, π–π interactions play a significant role in the solid-state arrangement of **2** only. In 2(DEB)·dpb, **3**, (dpb = 1,4-bis(4-pyridyl)-benzene), an alternative 2:1 DEB:bipyridyl stoichiometry is observed. Dimeric DEB hydrogen-bonded units are linked into hydrogen-bonded chains through further hydrogen bonding. The co-crystal DEB·pypm, **4**, (pypm = 5-(4-pyridyl)pyrimidine), also forms dimeric DEB hydrogen-bonded units which interact with the pyridyl groups of pypm. However, the pyrimidine groups of pypm do not participate in hydrogen bonding to DEB molecules and as a result discrete dimeric 2(DEB)·2(pypm) units are formed.

Keywords: hydrogen bond; tecton; barbituric acids

Introduction

One of the major themes that underpin crystal engineering is the use of supramolecular interactions, notably hydrogen bonds, to arrange molecules in the solid state (*1*). Hydrogen-bonding interactions have been extensively studied since the earliest developments of the field (*2*) and can be exploited to create increasingly intricate structural arrangements (*3*). Whilst other interactions, notably coordinate bonds (*4*), can be utilised in attempts to control molecular arrangements in crystalline materials, purely organic systems are most commonly designed utilising hydrogen bonds. Other supramolecular interactions such as halogen-bonding (*5*) and π–π stacking interactions (*6*) can also be exploited in attempts to influence long-range order.

We, amongst others, have been exploring crystal engineering using cyanuric acid (CA) (*7–10*), exploiting the potential of the imide moiety to form complementary triple hydrogen bonds with appropriate molecules. Our studies underpin extensive solution-based supramolecular chemistry exploiting such interactions (*11*) and more recent surface-based self-assembly processes (*12*). It is notable, particularly from solution-based studies (*11*), that barbituric acid derivatives such as 5,5-diethyl-barbituric acid (DEB) are capable of forming hydrogen bonds in a similar fashion to CA, but with only two, rather than three, imide moieties incorporated within the molecule. Surprisingly, few examples of crystal engineering using barbituric acids have been reported (*13–16*): these include the studies of pyridyl···barbituric acid N—H···N interactions (*13–15*) and the interactions between pyridine-N-oxides and barbituric acids (*16*).

We have previously studied the solid-state arrangements adopted by CA···bipyridyl co-crystals (*7–9*): typically such adducts form two-dimensional sheets with the bipyridyl species bridging $(CA)_\infty$ chains (*7,8*) or $(CA)_2$ dimers (*9*). Barbituric acids offer only two imide hydrogen-bonding sites in comparison with three of CA and are, therefore, expected to favour structures of lower dimensionality than those seen in the co-crystals of CA. This study illustrates that this is indeed the case, and one-dimensional chain structures are observed in the majority of cases studied. We have studied three relatively simple linear bipyridyl molecules, namely 4,4'-bipy, 2,7-diazapyrene (diaz) and 1,4-bis(4-pyridyl)-benzene (dpb; Scheme 1). All are capable of acting as hydrogen bond acceptors, and we have investigated not only the hydrogen-bonded motifs adopted but also the role of π–π stacking interactions in the aggregation of chains in the solid state. In addition to these linear bipyridyl molecules, we have investigated the hydrogen bond acceptor pypm (pypm = 5-(4-pyridyl)pyrimidine; Scheme 1), a molecule that contains both pyridyl and pyrimidine units. Although we anticipated interesting hydrogen-bonding interactions

---

*Corresponding author. Email: neil.champness@nottingham.ac.uk

ISSN 1061-0278 print/ISSN 1029-0478 online

http://dx.doi.org/10.1080/10610278.2011.622383
http://www.tandfonline.com

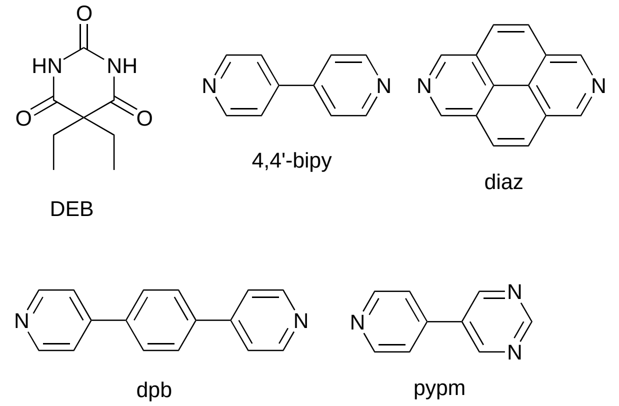

Scheme 1. Molecules employed in this study.

between the pyrimidine and barbituric acid groups, bearing in mind the compatible angles seen in both DEB and pypm, we were also mindful of the relative hydrogen bonding and coordinating capacity of pyrimidines and pyridines (*17*).

Results and discussion

Single crystals of co-crystals **1–4**, DEB·4,4'-bipy **1**, DEB·diaz **2**, 2(DEB)·dpb **3** and DEB·pypm **4**, were formed by slow evaporation to dryness of a methanol/*m*-xylene (*ca.* 15:1 v/v) solution of the two components. In the case of **1** and **2**, the hydrogen-bonded co-crystals crystallised as *m*-xylene solvates with the asymmetric unit containing one DEB molecule, one bipyridyl molecule [4,4'-bipy (**1**) or diaz (**2**)] and a disordered *m*-xylene molecule. Attempts to co-crystallise DEB with either 4,4'-bipy or diaz in the absence of *m*-xylene resulted only in the formation of microcrystalline material. Co-crystals **3** and **4** crystallise without solvation: only one DEB molecule and half a dpb molecule (**3**) or one pypm molecule (**4**) comprise the asymmetric unit. In all cases, hydrogen bonding is observed between the DEB molecules and the pyridyl moieties of the co-crystallised base. However, the nature of this hydrogen bonding varies depending on the specific co-crystal, and **3** and **4** illustrate that competitive inter-barbituric acid N—H···O hydrogen bonding is also important in determining the resultant hydrogen-bonded structure.

The structures of **1** and **2** comprise layers of one-dimensional chains of alternating DEB and bipyridyl molecules (Figure 1), with each N—H group of the DEB molecules forming a N—H···N hydrogen bond to a pyridyl nitrogen of 4,4'-bipy (**1**) or diaz (**2**) (Figure 2, Table 1). The N—H···N hydrogen bonds between the DEB and 4,4'-bipy molecules are comparable in length to related systems (*7,9*), with an average N···N separation of 2.85 Å in **1** and 2.87 Å in **2**. The NH···N hydrogen bonds are supplemented by weaker C—H···O interactions between the C—H groups *ortho* to the N donors of 4,4'-bipy in **1** or diaz in **2** and the acceptor carbonyl oxygen groups on DEB. Although in **1** the C—H···O interactions are facilitated by the twist in the 4,4'-bipy molecule (torsion angle 34°) which allows the C—H groups on 4,4'-bipy to be in an optimal position for the weaker hydrogen bonds to form, in the case of **2** the planar nature of diaz enforces a highly planar arrangement for the DEB·diaz chain. Inspection of the C = O and C—N bond lengths of the DEB molecule in **1** or **2**, and comparison with previously reported data (*18*), indicates that the hydrogen bonding between DEB and 4,4'-bipy has no significant effect upon these bond lengths within DEB.

In **1**, hydrogen-bonded chains of DEB·4,4'-bipy form layers which stack in such a way as to generate cavities between the layers. These cavities are occupied by *m*-xylene molecules which are disordered across crystallographic inversion centres (Figure 3(a,b)), with π–π stacking interactions between 4,4'-bipy and *m*-xylene (interplanar angle = 5.3°; centroid–centroid distances between *m*-xylene···pyridyl range between 3.4 and 3.6 Å). In contrast to **1**, in **2** the stronger preference for diaz···diaz π–π stacking interactions (diaz···diaz centroid–centroid separation 3.96 Å, interplanar angle 2.7°) leads to the formation of stacks of DEB·diaz chains (Figure 3(c–e)). The resulting cavities between sheets in **2** are occupied by *m*-xylene molecules.

It is clear from these two structures that intermolecular π–π stacking interactions between diaz molecules are more favoured than those between 4,4'-bipy molecules, significantly affecting the long-range ordering of chains in **2**. Figure 3(e) clearly illustrates the extended π–π interactions of diaz molecules to form stacks, resulting in the formation of sheets of DEB·diaz chains. The sheets are capped by the DEB ethyl groups, leaving cavities that are occupied by guest *m*-xylene molecules. In contrast to **2**, the sheets formed by **1** do not exhibit extended π–π interactions between 4,4'-bipy molecules; instead, adjacent DEB·4,4'-bipy chains are separated by included *m*-xylene molecules. Furthermore, the presence of π–π interactions between diaz molecules influences the relative orientation of adjacent chains in **2** in comparison with **1**. Thus, adjacent DEB·diaz chains in **2** undulate in such a manner that adjacent chains are displaced by half a repeat unit (Figure 3(c)), whereas adjacent DEB·4,4'-bipy chains in **1** are not displaced (Figure 3(b)). The differences in orientation arise from the closer proximity of chains in **2**, resulting from the diaz···diaz π–π interactions, and require the out-of-phase orientation to prevent clashing between the ethyl substituents of the DEB molecules. The influence of π–π interactions between diaz molecules in the extended structures has been noted previously in coordination polymer architectures (*19*).

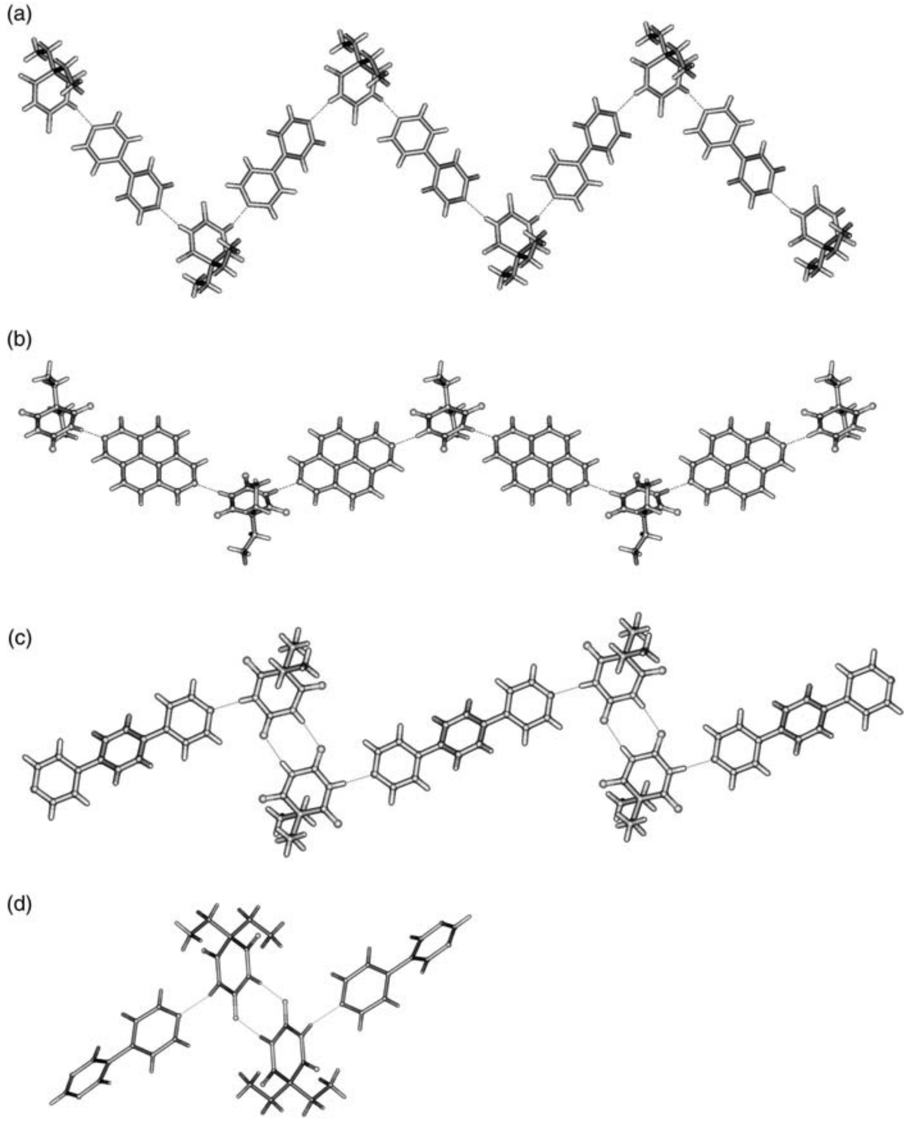

Figure 1. Views of the chains of (a) **1**, (b) **2** and (c) **3**. (d) the discrete hydrogen-bonded dimeric unit formed by **4**.

Similar to **1** and **2**, **3** forms hydrogen-bonded chains composed of DEB and the bipyridyl molecule, dpb. However, in contrast to **1** and **2**, **3** has a different stoichiometry, 2(DEB)·dpb, and as a result exhibits a different hydrogen-bonding arrangement (see Table 1 for pertinent hydrogen bonds details). In particular, inter-DEB N—H···O hydrogen bonding is observed with the formation of an imide···imide interaction which can be described using the graph-set notation $R_2^2(8)$ (*20*) (Figure 1(c)). Thus, DEB–DEB dimeric units are observed which offer N—H donors on opposing sides, similar to the CA dimers observed in CA·diaz (*9*), which are in turn hydrogen bonded to two separate dpb molecules *via* N—H···N interactions. As in **1**, no significant π–π interactions are observed between adjacent 2(DEB)·dpb chains, with the shortest such interactions occurring between dpb molecules in adjacent chains (centroid–centroid separation of 4.3 Å, interplanar angle 38°). Despite the presence of *m*-xylene in the solvent mixture used for crystallisation, it is not included in the structure of **3**. The precise reason for this is unclear but presumably reflects a greater packing efficiency in the observed structure in comparison with a hypothetical alternative *m*-xylene solvate of **3**.

Co-crystal **4** resembles **3** in that it contains DEB–DEB dimeric units assembled *via* $R_2^2(8)$ imide···imide interactions *via* N—H···N hydrogen bonds to the pyridyl moiety of pypm (Figure 1(d)). However, unlike the N-donor bases in **1**–**3**, pypm does not act as a conventional hydrogen-bonding bridge and the pyrimidine group does not participate in N—H···N hydrogen bonds. Thus, 2(DEB)·2(pypm) dimeric units are formed which associate

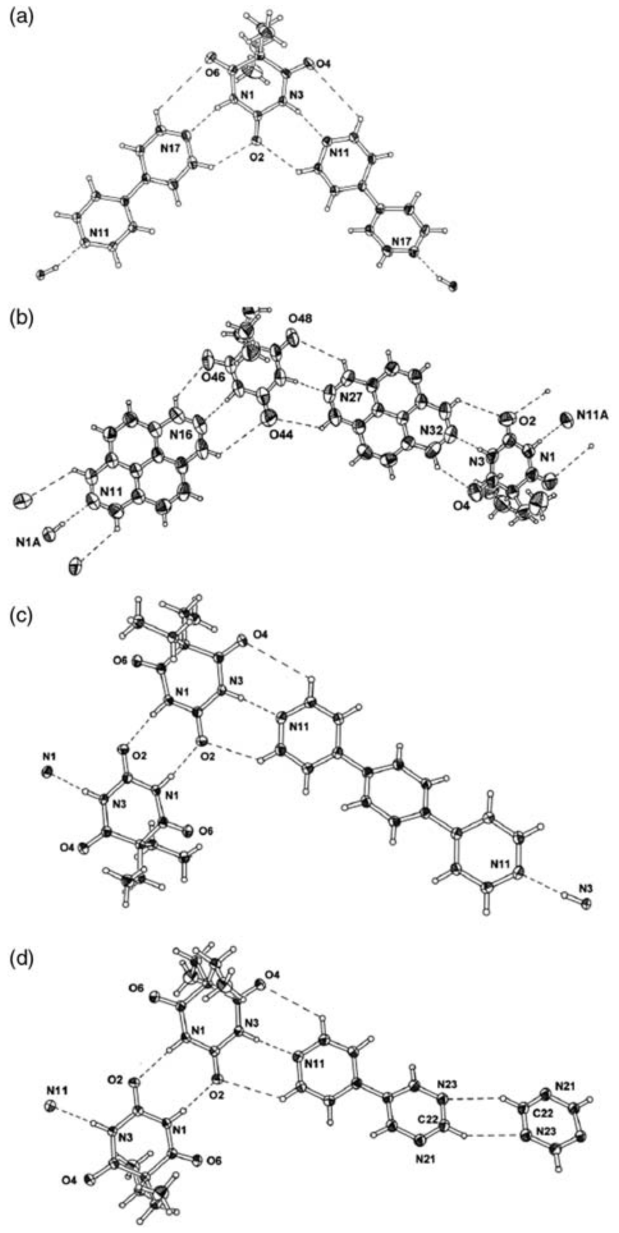

Figure 2. Hydrogen-bonding interactions observed in the asymmetric units of (a) **1**, (b) **2**, (c) **3** and (d) **4**. Displacement ellipsoids are drawn at the 50% probability level.

with extended chains *via* C—H···N hydrogen bonds (Table 1) between pyrimidine groups in adjacent dimers (Figure 4).

Both face-to-face π–π stacking and edge-to-face C—H···π interactions are observed in **4** (Figure 5). Face-to-face π–π stacking interactions occur between pyrimidine rings of adjacent 2(DEB)·2(pypm) dimeric units (pyrimidine···pyrimidine centroid–centroid separation of 3.61 Å, interplanar angle 0°) and are accompanied by edge-to-face C—H···π interactions between the opposing face of each pyrimidine ring and the pyridine rings of a third 2(DEB)·2(pypm) dimeric unit [C—H(pyridine)···centroid(pyrimidine) = 3.04 Å; < C—H···centroid(pyrimidine) = 97.2°) (*21*).

All four co-crystals were studied by powder X-ray diffraction (PXRD) in order to assess whether a single product was produced from the reactions. Bulk samples were prepared by precipitation from MeOH and *m*-xylene. Unfortunately, PXRD studies of ground samples revealed that the samples had low crystallinity (see Supplementary Information available online). Those peaks observed were largely consistent with the single crystal structures, particularly in the case of **1**. However, samples of **2**–**4** gave patterns showing poorer agreement with patterns simulated from the corresponding single crystal data: samples **2**–**4** clearly contain additional phases. Two phases have been reported for DEB, one trigonal (*22*) and one monoclinic (*23*), and these appear to be amongst the additional phases present in the bulk samples. Despite our inability to prepare bulk samples of **2**–**4**, we are still able to prepare single crystals of these materials and separate them manually from the other products of crystallisation where required. The effect of grinding on the samples, if any, is unclear and it should be borne in mind the well-established fact that grinding can induce phase changes in co-crystals (*24*).

Conclusions

In conclusion, we have shown that bidentate bipyridyl-based molecules can be successfully exploited to form hydrogen-bonded chains with DEB. In three cases, **1**–**3**, one-dimensional hydrogen-bonded chains are observed in which N—H···N interactions between pyridyl moieties and N—H groups of DEB result in chains. Subtle differences are found between these three related co-crystals, with **1** and **2** displaying similar motifs for 1:1 DEB:bipyridyl stoichiometry. Comparison of **1** with **2** shows that well-defined intermolecular π–π interactions between diaz molecules affect the relative orientation of adjacent hydrogen-bonded chains. In contrast, despite analogous crystallisation conditions, **3** adopts a 2:1 DEB:bipyridyl stoichiometry, resulting in the formation of dimeric DEB–DEB hydrogen-bonded units which are propagated into one-dimensional chains *via* N—H···N hydrogen bonds between DEB and dpb. The self-association of DEB molecules is unsurprising in light of previous studies of CA in the solid state (*9*), and of solution phase studies which have demonstrated self-association of DEB in the presence of relatively weak pyridyl-based hydrogen bond acceptors (*25*).

The introduction of a potential alternative hydrogen-bonding acceptor in the form of a pyrimidine group in combination with a pyridine group, through the incorporation of pypm into a hydrogen-bonded co-crystal in **4**, offers an interesting comparison with **1**–**3**. It is notable

Table 1. Selected hydrogen bond parameters observed in **1**–**4**.

D—H···A	*d*(D—H) (Å)	*d*(H···A) (Å)	*d*(D···A) (Å)	<(DHA) (°)
1				
N1—H1···N17	0.88	1.99	2.847(2)	165
N3—H3···N11^a	0.88	1.99	2.859(3)	167
N11—H11···N3^b	0.88	2.02	2.859(2)	158
2				
N3—H3···N32	0.88	1.99	2.866(3)	175
N1—H1···N11^c	0.88	1.99	2.865(3)	173
N43—H43···N27	0.88	1.99	2.869(3)	176
N45—H45···N16	0.88	2.00	2.878(3)	177
3				
N1—H1···O2^d	0.88	1.99	2.861(2)	173
N3—H3···N11	0.88	1.92	2.802(2)	175
4				
N1—H1···O2^e	0.88	2.02	2.892(1)	174
N3—H3···N11^f	0.88	1.97	2.799(2)	156
C22—H22···N23^g	0.95	2.60	3.465(2)	152

Symmetry transformations used to generate equivalent atoms: ^{a} $-1/2+x, -1/2-y, -1/2+$,I; ^{b} $z+1/2, -y-1/2, z+1/2$; ^{c} $x+1, y, z$; ^{d} $1-x, -y, 1-z$; ^{e} $-x, 2-y, -z$; ^{f} $1+x, 1+y, z$; ^{g} $2-x, 1-y, 1-z$.

that in **4**, DEB preferentially hydrogen bonds to the pyridine moiety instead of the pyrimidine group, thereby forming discrete dimeric groups.

We have successfully demonstrated the capacity of DEB to act as a versatile hydrogen-bonding tecton in the crystalline state. It is clear that DEB–DEB hydrogen bonding, and the resultant formation of hydrogen-bonded dimers as seen in **3** and **4**, represents a significant barrier to the controlled design of solid-state supramolecular structures. We are currently developing this methodology to further advance our understanding of hydrogen-bonded architectures in the solid state.

Experimental

All chemicals were purchased from Aldrich Chemical Company, UK, and used without further purification, except for diaz (*26*), dpb (*27*) and pypm (*28*) which were prepared following literature procedures. Elemental analyses were performed by Stephen Boyer, London Metropolitan University, London, UK. Infrared spectra were obtained (solid state) using a Nicolet Avatar 360 FTIR spectrometer.

1. DEB (5 mg, 0.03 mmol) and 4,4'-bipy (4.2 mg, 0.03 mmol) were dissolved in methanol (15 cm^3) with two drops of *m*-xylene and the resulting solution was left to evaporate. Crystals grew over a period of *ca.* 1 week following evaporation of the solution. Found (calculated for $C_{22}H_{25}N_4O_3$) C 66.92 (66.82), H 6.16 (6.26), N 14.50 (14.62) %. IR υ(cm^{-1}) 2974(w), 2769(w), 1736(s), 1705(s), 1680(s), 1593(m), 1460(m), 1408(m), 1374(m), 1309(m), 1218(m), 1103(m), 1071(m), 999(w), 812(m), 794(m).

2. DEB (2.2 mg, 0.01 mmol) and diaz (2.5 mg, 0.01 mmol) were dissolved in hot methanol (15 mL) with two drops of *m*-xylene. The solvent was allowed to evaporate from the resulting solution and crystals grew over a period of *ca.* 1 week. Although single crystals could be separated manually from the bulk, PXRD studies and elemental analysis have shown that the bulk sample is contaminated by at least one other phase. IR υ(cm^{-1}) 3854(w), 2786(w), 1740(m), 1709(m), 1700(m), 1458(m), 1413(m), 1316(m), 1237(s), 1149(m), 1033(m), 983(m), 899(m), 717(m). Found (calculated for $C_{26}H_{25}N_4O_3$; (DEB)• or ·(diaz)• or ·(*m*-xylene)$_{0.5}$) C 70.73 (70.79), H 5.71 (5.65), N 12.69 (12.74).

3. DEB (2.2 mg, 0.01 mmol) and dpb (2.3 mg, 0.01 mmol) were dissolved in hot methanol (15 mL) with two drops *m*-xylene and the resulting solution was left to evaporate. Crystals grew over a period of *ca.* 1 week. Although single crystals could be separated manually from the bulk, PXRD and elemental analyses have shown that the bulk sample is contaminated by at least one other phase.

4. DEB (2.2 mg, 0.01 mmol) and pypm (1.6 mg, 0.01 mmol) were dissolved in hot methanol (15 mL) with two drops *m*-xylene and the resulting solution was left to evaporate. Crystals grew over a period of *ca.* 1 week. Although single crystals could be separated manually from the bulk, PXRD and elemental analysis have shown that the bulk sample is contaminated by at least one other phase.

Single crystal X-ray experiments were performed either on a Bruker AXS SMART APEX CCD area detector diffractometer (**1**,**3**) or on a Bruker AXS SMART1000 CCD area detector diffractometer (**2**,**4**) [graphite-monochromated Mo-K$_\alpha$ radiation ($\lambda = 0.71073$ Å); ω scans], each equipped with an Oxford Cryosystems open-flow cryostat (*29*). All structures were solved by direct methods using SHELXS97 (*30*) and all non-H atoms were located using subsequent difference Fourier methods and were

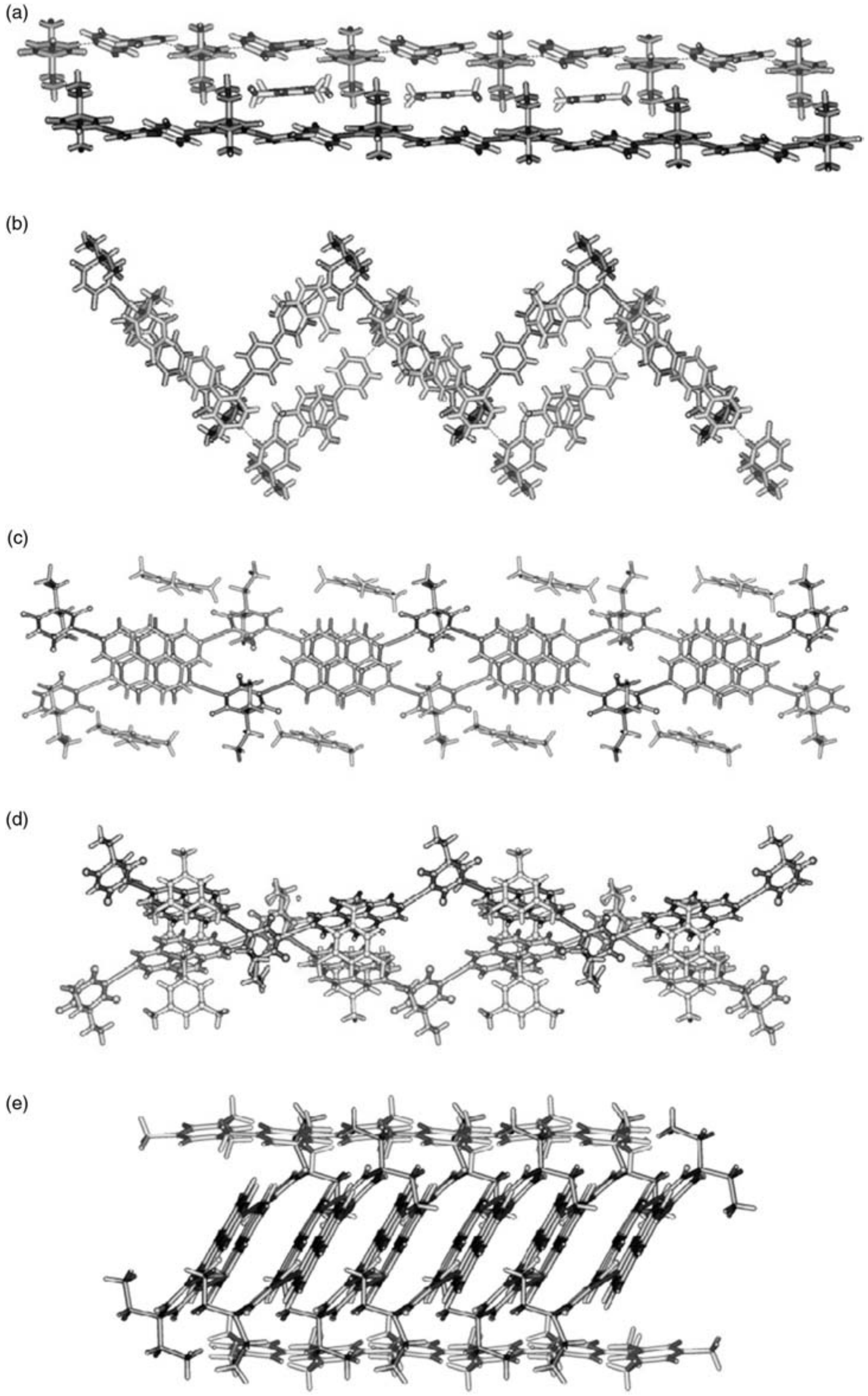

Figure 3. (a,b) Views along the crystallographic *b*-axis (a) and *a*-axis (b) of the long-range order observed in hydrogen-bonded chains of **1**, with *m*-xylene molecules positioned in cavities between 4,4'-bipy molecules. (c,d) Views along the crystallographic *b*-axis (c) and *c*-axis (d) of two hydrogen-bonded chains of **2** and *m*-xylene molecules. (e) View along the crystallographic *a*-axis of **2**: note the π–π stacking interactions between diaz molecules of adjacent one-dimensional chains.

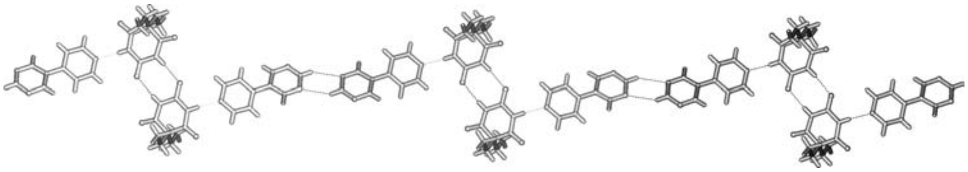

Figure 4. View of the association of adjacent 2(DEB)·2(pypm) dimeric units with extended chains *via* pyrimidine···pyrimidine C—H···N hydrogen bonds.

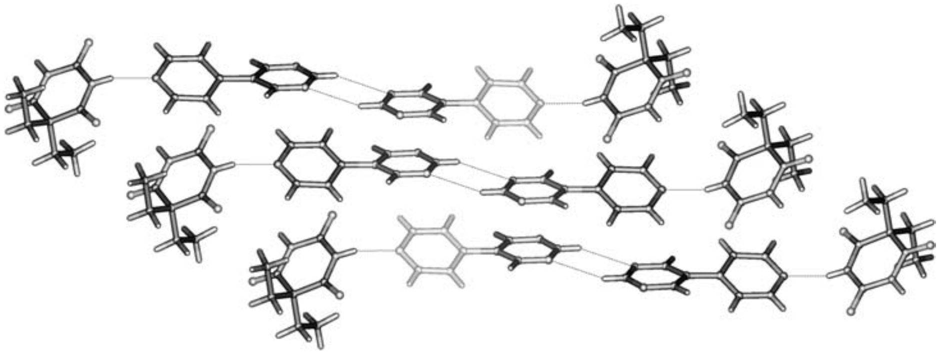

Figure 5. View of the π–π stacking interactions observed in **4**. Face-to-face π–π stacking interactions between adjacent pyrimidine rings. In addition edge-to-face C—H···π interactions are observed between pyridine rings (light grey) and pyrimidine rings (dark grey).

refined with anisotropic displacement parameters. Except where noted below, hydrogen atoms were first located in electron difference maps, then placed in geometrically calculated positions and thereafter allowed to ride on their parent atoms. For **1** the *m*-xylene molecule was found to be disordered such that the two methyl groups are distributed over three sites: in refinement, the sum of the three occupancies was restrained to a value of 2.00(1). A consequence of this model is that one hydrogen atom is disordered across three sites: this has not been included in the refinement model leading to a discrepancy between the calculated and reported formulae. In **2**, the DEB ethyl groups C49/C50 and C51/C52 are each disordered over two orientations with the sum of the occupancies for each

Table 2. Summary of crystallographic data.

	1	**2**	**3**	**4**
Chemical formula	$C_{22}H_{25}N_4O_3$	$C_{52}H_{52}N_8O_6$	$C_{32}H_{36}N_6O_3$	$C_{17}H_{19}N_5O_3$
M	393.46	885.02	600.67	341.37
Crystal system	Monoclinic	Monoclinic	Triclinic	Triclinic
Space group	$P2_1/n$	$P2_1/c$	$P-1$	$P-1$
a (Å)	11.4278(10)	26.651(3)	6.5893(6)	6.6679(5)
b (Å)	8.9406(8)	7.9661(9)	10.5540(1)	11.5658(8)
c (Å)	20.3519(19)	22.563(3)	11.681(1)	11.8681(8)
α (°)	–	–	105.812(2)	102.189(1)
β (°)	93.618(2)	105.661(2)	102.486(2)	102.307(1)
γ (°)	–	–	103.112(2)	98.912(1)
V (Å)^3	2075.2(3)	4612.5(9)	727.0(1)	854.7(1)
Z	4	4	1	2
T (K)	150(2)	150(2)	150(2)	150(2)
μ (mm^{-1})	0.086	0.085	0.097	0.094
Reflections collected	17860	38743	6579	7737
Unique reflections (R_{int})	4766 (0.081)	10466 (0.113)	3292 (0.034)	3840 (0.029)
Goodness of fit	1.03	0.98	1.01	1.04
$\Delta\rho_{max}$, $\Delta\rho_{min}$ (eÅ^{-3})	0.34, −0.26	0.42, −0.28	0.31, −0.27	0.31, −0.23
Final R_1 [$F > 4\sigma(F)$]	0.0621	0.0628	0.0423	0.0370
wR_2 (all data)	0.130	0.173	0.0987	0.105

respective pair of chains restrained to unity. Appropriate restraints have been applied to the geometric and displacement parameters of the atoms involved. The xylene solvent moiety is disordered over three possible orientations related to rotation through 120° about the centroid of the phenyl ring. The occupancies of the three possible sites for the methyl groups have been restrained to 2.00(1). Appropriate restraints and constraints were applied to the geometric and displacement parameters of the molecule. In contrast, no disorder was encountered in either **3** or **4**. Crystal data and other experimental details are summarised in Table 2. CCDC 654154 (**1**), CCDC 654155 (**2**), CCDC 699235 (**3**) and CCDC 699236 (**4**) contain the supplementary crystallographic data for this paper. These data can be obtained free of charge from the Cambridge Crystallographic Data Centre via http://www.ccdc.cam.ac.uk/data_request/cif.

Acknowledgements

We would like to gratefully acknowledge the support of the Engineering and Physical Sciences Research Council. NRC gratefully acknowledges receipt of a Royal Society Leverhulme Trust Senior Research Fellowship.

References

(1) (a) Steiner, T. *Angew. Chem. Int. Ed.* **2002**, *41*, 48–76. (b) Desiraju, G.R. *Acc. Chem. Res.* **2002**, *35*, 565–573. (c) Aakeröy, C.; Champness, N.R.; Janiak, C. *CrystEngComm.* **2010**, *12*, 22–43. (d) Friscic, T.; Jones, W. *Cryst. Growth Des.* **2009**, *9***,** 1621–1637. (e) Dunitz, J.D.; Gavezzotti, A. *Chem. Soc. Rev.* **2009**, *38*, 2622–2633. (f) Aakeroy, C.B.; Salmon, D.J. *CrystEngComm.* **2005**, *7***,** 439–448. (g) Aakeroy, C.B. *Acta Cryst. Sect. B* **1997**, *53*, 569–586. (h) Aakeroy, C.B.; Seddon, K.B. *Chem. Soc. Rev.* **1993**, *22*, 397–407. (h) Jia, J.; Hubberstey, P.; Champness, N.R.; Schröder, M. *Struct. Bonding*, **2009**, *132*, 135–161. (g) Macgillivray, L.R.; Papaefstathiou, G.S.; Friscic, T.; Hamilton, T.D.; Bucar, D.-K.; Chu, Q.; Varshney, D.B.; Georgiev, I.G. *Acc. Chem. Res.* **2008**, *41*, 280–291.

(2) Etter, M.C. *Acc. Chem. Res.* **1990**, *23*, 120–126 and references therein.

(3) (a) Maly, K.E.; Gagnon, E.; Maris, T.; Wuest, J.D. *J. Am. Chem. Soc.* **2007**, *129*, 4306–4322. (b) Ward, M.D. *Chem. Commun.* **2005**, 5838–5842. (c) Hamblin, J.; Argent, S.P.; Blake, A.J.; Wilson C.; Champness, N.R. *CrystEngComm.* **2008**, *10*, 1782–1789. (d) Yang, W.; Greenaway, A.; Lin, X.; Matsuda, R.; Blake, A.J.; Wilson, C.; Lewis, W.; Hubberstey, P.; Kitagawa, S.; Champness, N.R.; Schröder, M.*J. Am. Chem. Soc.* **2010**, *132*, 14457–14469.

(4) (a) Blake, A.J.; Champness, N.R.; Hubberstey, P.; Li, W.-S.; Withersby, M.A.; Schröder, M. *Coord. Chem. Rev.* **1999**, *183*, 117–138. (b) Hill, R.J.; Long, D.-L.; Champness, N.R.; Hubberstey, P.; Schröder, M. *Acc. Chem. Res.* **2005**, *38*, 337–350.

(5) Cavallo, G.; Metrangolo, P.; Pilati, T.; Resnati, G.; Sansotera, M.; Terraneo, G. *Chem. Soc. Rev.* **2010**, *39*, 3772–3783.

(6) Janiak, C. *J. Chem. Soc. Dalton Trans.* **2000**, 3885–3896.

(7) Barnett, S.A.; Blake, A.J.; Champness, N.R. *CrystEngComm* **2003**, *5*, 134–136.

(8) Ranganathan, A.; Pedireddi, V.R.; Sanjayan, G.; Ganesh, K.N.; Rao, C.N.R. *J. Mol. Struct. (THEOCHEM)* **2000**, *522*, 87–94.

(9) Ring, D.J.; Blake, A.J.; Champness, N.R.; Wilson, C. *CrystEngComm* **2006**, *8*, 29–32.

(10) MacDonald, J.C.; Whitesides, G.M. *Chem. Rev.* **1994**, *94*, 2383–2420.

(11) Whitesides, G.M.; Simanek, E.E.; Mathias, J.P.; Seto, C.T.; Chin, D.N.; Mammen, M.; Gordon, D.M. *Acc. Chem. Res.* **1995**, *28*, 37–44.

(12) (a) Theobald, J.A.; Oxtoby, N.S.; Phillips, M.A.; Champness, N.R.; Beton, P.H. *Nature*, **2003**, *424*, 1029–1031. (b) Perdigão, L.M.A.; Champness, N.R.; Beton, P.H. *Chem. Commun.* **2006**, 538–540. (c) Slater (neé Phillips), A.G.; Beton, P.H.; Champness, N.R. *Chem. Sci.* **2011**, *2*, 1440–1448.

(13) Vishweshwar, P.; Thaimattam, R.; Jaskolsi, M.; Desiraju, G.R. *Chem. Commun.* **2002**, 1830–1831.

(14) Hsu, I.-N.; Craven, B.M. *Acta Crystallogr. Sect B.* **1974**, *30*, 994–997.

(15) Haixin, L.; Xin, W.; Xinmin, Z. *Acta Crystallogr. Sect. C* **1992**, *48*, 2096–2098.

(16) Reddy, L.S.; Babu, N.J.; Nangia, A. *Chem. Commun.* **2006**, 1369–1371.

(17) Aakeroy, C.B.; Schultheiss, N.; Desper, J.; Moore, C. *Cryst. Growth Des.* **2007**, *7*, 2324–2331.

(18) Craven, B.M.; Cusatis, C.; Gartland, G.L.; Vizzini, E.A. *J. Mol. Struct.* **1973**, *16*, 331–342.

(19) (a) Blake, A.J.; Champness, N.R.; Khlobystov, A.N.; Lemenovskii, D.A.; Li, W.-S.; Schröder, M. *Chem. Commun*. **1997**, 1339–1340. (b) Blake, A.J.; Baum, G.; Champness, N.R.; Chung, S.S.M.; Cooke, P.A.; Fenske, D.; Khlobystov, A.N.; Lemenovskii, D.A.; Li, W.-S.; Schröder, M.J. *Chem. Soc. Dalton Trans*. **2000**, 4285–4291.

(20) Etter, M.C. *Acc. Chem. Res.* **1990**, *23*, 120–126.

(21) Nishio, M. *CrystEngComm* **2004**, *6*, 130–158.

(22) Craven, B.M.; Vizzini, E.A.; Rodrigues, M.M. *Acta Crystallogr. Sect. B* **1969**, *25*, 1978–1993.

(23) McMullan, R.K.; Fox, Jr., R.O.; Craven, B.M. *Acta Crystallogr. Sect. B* **1978**, *34*, 3719–3722.

(24) Trask, A.V.; Jones, W. *Top. Curr. Chem.* **2005**, *254*, 41–70.

(25) Mason, P.V.; Champness, N.R.; Collinson, S.R.; Fisher, M.G.; Goretzki, G. *Eur. J. Org. Chem.* **2006**, 1444–1449.

(26) Hunig, S.; Gross, J.; Lier, E.F.; Quast, H. *Liebigs Ann. Chem.* **1973**, 339–358.

(27) Biradha, K.; Fujita, M. *J. Chem. Soc. Dalton Trans.* **2000**, 3805–3810.

(28) Thébault, F.; Barnett, S.A.; Blake, A.J.; Champness, N.R.; Schröder, M.; Wilson, C. *Inorg. Chem.* **2006**, *45*, 6179–6187.

(29) Cosier, J.; Glazer, A.M. *J. Appl. Crystallogr.* **1986**, *19*, 105–107.

(30) Sheldrick, G.M. *Acta Crystallogr. Sect. A* **2008**, *64*, 112–122.